



Evaluation of corrosion inhibitive properties of *Trigonella foenum-graecum* for pure Aluminium in hydrochloric acid

D.G. Ladha¹, P.M. Wadhvani¹, S. Kumar¹, N.K. Shah^{1*}

¹Department of Chemistry, School of Sciences, Gujarat University, Navrangpura, Ahmedabad-380009, Gujarat, India

Received 24 Aug 2014; Revised 23 Sept 2014; Accepted 23 Sept 2014.

*Corresponding Author; Email: nishchem2004@yahoo.co.in

Abstract

Water extract of fenugreek seeds (*FSE*) were assessed for its corrosion inhibitory activity on Aluminium (Al) in 1.0 M hydrochloric acid (HCl) solution. The inhibitive effect of fenugreek extract was studied using gravimetric, galvanostatic polarization and electrochemical impedance spectroscopy techniques. The results show that presence of *FSE* reduces the corrosion rate of Al due to the action of phytochemical constituents such as Trigonelline and Vitexin present in it, as obtained from Liquid chromatography-Mass spectrometry (LC-MS) analysis. The corrosion process was inhibited by the adsorption of extract molecules over metal surface and was found to follow Langmuir adsorption isotherm.

Keywords: Green corrosion inhibitor, Aluminum, HCl, DFT, Electrochemical and Gravimetric methods

1. Introduction

Trigonella foenum-graecum (fenugreek) belongs to the subfamily Papilionaceae of the family Leguminosae. The plant is an aromatic herbaceous annual, widely cultivated in Mediterranean countries and Asia. In India, its cultivation is concentrated mainly in Rajasthan which contributes 80% of the total area as well as production. Fenugreek seed is used as a spice in culinary preparation. In most cases, the whole seeds are used. When separated into testa and albumen, fenugreek has completely different functions. The seed consists of 75% testa and 25% albumen; the testa contains fragrant essential oil, saponin, protein and it functions as a spice. On the other hand, albumen consists of 80% water-soluble and 20% water insoluble substance. The seeds are rich source of polysaccharide substance named galactomannan and various phytochemical constituents (volatile and non-volatile). The volatile components of seed are: cadinene, cadinol, bisabolol, linoleic, oleic and linolenic acid. The non-volatile components isolated from fenugreek include steroids, fatty acids and flavonoids. Sterols, diosgenin derivatives and trigonellin are the most important among the non-volatiles. Fenugreek has been used extensively in various medicinal preparations. Fenugreek seeds and leaves are anti-cholesterolemic, anti-inflammatory, antitumor, carminative, demulcent, deobstruent, emollient, expectorant, febrifuge, galactagogue, hypoglycaemic, laxative, parasiticide, restorative and uterine tonic, and useful in burning sensation [1, 2].

The area of research for fenugreek seeds can be enhanced from medicinal purposes to corrosion inhibitor. The basic criteria to be a corrosion inhibitor is presence of heteroatoms (N, O, S) and π -electrons [3-10] which is fulfilled by the phytochemical constituents present in fenugreek seeds. Various steps are taken to explore the fenugreek application in the field of corrosion science due to the presence of naturally synthesized organic compounds [11]. However, in previous researches fenugreek seed is used as a corrosion inhibitor for mild steel [12, 13].

The present study is focused on the evaluation of fenugreek seed extract (*FSE*) as a corrosion inhibitor for pure Aluminium (Al) in presence of 1.0 M hydrochloric acid solution. The investigation is fulfilled with the help of gravimetric, galvanostatic polarization and electrochemical impedance techniques. Further, LC-MS analysis of *FSE* is undertaken to detect the inhibitory molecules present in the extract. The objective of the study is to get insight

into the mechanism of inhibitor molecules adsorption when added to the corrosive environment to understand the metal/corrosion interaction [14-18].

2. Experimental section

2.1. Preparation and characterization of FSE

The stock solution of inhibitor is prepared by immersing weighed amount of fenugreek grounded seeds in water for 24 hours and then filtered. Inhibitor test solutions are prepared, with its concentration varying from 0.024 g/l-0.939 g/l, by diluting the stock solution of extract in 1.0 M HCl solution.

LC-MS analysis of FSE is performed using WATERS make HPLC-2695 to know the chemical constituents present in the extract. The column used is X-bridge 5 μ m C-18 of 100x4.6mm. The mobile phase used is 0.1% formic acid in water (A) and 100% methanol (B). The sample is injected with a flow rate of 1ml/minute with an injection volume of 10 μ l. Waters QDa Mass Detector with Single Quadra pole with ionization technique is used for the detection of the components molecular weight. The identification of molecules was performed using literature survey [2].

2.2. Gravimetric method

Tests were performed on Al specimen with composition Al (99.2%), Fe (0.498%), Si (0.144%), Mn (0.031%), Cu (0.007%), Mg (0.005%) and Zn (0.001%). The measurements were conducted on Al (3.0 \times 6.0 \times 0.05 cm) in presence and absence of inhibitor in 1.0 M HCl solution. The specimens were abraded with emery, degreased with acetone and stored in desiccator prior to use for the gravimetric measurements. The measurements were carried out for Al specimen in 230 ml of 1.0 M HCl in presence and absence of different concentrations (0.024 g/l-0.939 g/l) of the inhibitor for exposure period of 1 hour respectively at 308 K. The temperature effect was also studied at 308 K, 318 K, 328 K and 338 K for the exposure period of 1 hour. They were then washed thoroughly with distilled water, dried and weighed by using Metler balance – M5 type.

2.3. Electrochemical method

A conventional three electrode cell was used with Al as working, platinum as counter and calomel as reference electrode. The specimens used for the measurement had diameter of 2.802 cm along with a handle of 3.0 cm long and 0.5 cm wide with a thickness of 0.087 cm and a small hole of about 2.0 mm just near the upper end of it. The circular portion with surface area of 6.156 cm² was exposed to the test solution in polarization studies. For impedance studies, calculations were performed for 1cm² surface area of specimen.

The potential was measured against a saturated calomel electrode in polarization study. The corrosion parameters such as; corrosion potential (E_{corr}), corrosion current density (I_{corr}) and Tafel slope (b_a, b_c) were measured by galvanostatic polarization method. In this study current density was varied in the range from 2×10^{-4} to 3.25×10^{-2} A/cm² and potential was calculated. The graph was plotted between log of current density (log I in A/cm²) and potential (E in mV) in order to determine the Tafel slopes.

Electrochemical impedance measurements (EIS) were carried out in the frequency range of 10kHz-1Hz. The open circuit potential was measured after 30 minutes of immersion of electrode in test solution by applying amplitude of 10 mV sine wave ac signal. EIS data were analyzed using frequency response analyzer (FRA) electrochemical setup in AUTOLAB instrument.

3. Results and Discussions

3.1. Characterization of FSE

There are nine compounds separated from LC-MS analysis but only three compounds are identified as shown in Table 1 and Figure 1. The identified compounds are: 1-Methylpyridinium-3-carboxylate (Trigonelline), 2-isobutyl 3-methoxy pyrazine (IBP) and Apigenin-8-C-glucoside (Vitexin). The presence of some carbohydrate compound was confirmed by testing the extract using Molish reagent and adding sulphuric acid sideways of test tube leading to formation of purple layer between acid and extract interface. However, structure of the carbohydrate cannot be confirmed by LC-MS analysis. In addition, the literature review shows the presence of pyrazine compound in fenugreek due to which it was approximated that the pyrazine may be IBP. Although V.A.Parthasarathy, B. Chempakam and T.J.Zachariah in their book named *Chemistry of spices* confirms the presence of Trigonelline and Vitexin in FSE.

3.2. Gravimetric measurements

3.2.1. Effect of concentration

The corrosion inhibition of Al in 1.0 M HCl solution at 308 K containing various concentrations of FSE was studied by measuring loss in weight of Al specimen. The data obtained from the measurement as shown in Table 2 reveals

that there is increase in efficiency of inhibitor when concentration is enhanced. There is an increase in efficiency of inhibitor from 10.296 % to 82.837% when concentration varies from 0.024 g/l-0.939 g/l for the exposure period of one hour. The enhancement in inhibition efficiency with respect to extract concentration suggests that more molecules were needed to adequately cover the metal surface when the concentration of inhibitor is low.

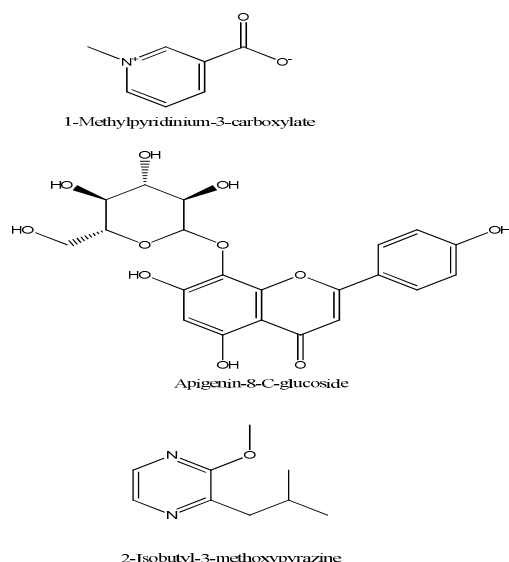


Figure 1: Main chemical constituents of *FSE*

Table 1:GC-MS analysis of *FSE* water extract

Peak	Retention Time (minutes)	Area (%)	Name
1	1.136	36.060	1-Methylpyridinium-3-carboxylate
2	2.757	1.280	2-isobutyl-3-methoxypyrazine
3	3.760	10.990	Apigenin-8-C-glucoside

Table 2:Corrosion parameters for pure Al in presence and absence of *FSE* at 308 K for exposure period of 60 minutes

Inhibitor	Inhibitor concentration, C(g/l)	Weight loss mgcm ⁻²	Surface coverage (θ)	Inhibition efficiency I. E%
Blank	-	23.68	-	-
<i>FSE</i>	0.024	21.246	0.103	10.277
	0.094	14.471	0.389	38.877
	0.187	11.382	0.411	41.062
	0.375	8.536	0.640	63.951
	0.469	7.317	0.691	69.100
	0.563	6.260	0.736	73.564
	0.657	6.260	0.736	73.564
	0.939	4.065	0.828	82.834

Further increase in concentration did not cause any appreciable change in the performance of the inhibitor thereby indicating the attainment of the limiting value. This effect may be due to the accumulation of the inhibitor molecules onto the positively charged metal surface, which reduces the direct contact of the metal and the corrosive environment. The higher performance of the *FSE* is attributed to the presence of carbon, oxygen atoms and larger

molecular size. The results so obtained are due to increase in surface coverage area of Al by inhibitor with increase in its concentration [19]. The inhibition efficiency and surface coverage is calculated by using equations 1 and 2 respectively.

$$\%I.E = \frac{W_u - W_i}{W_u} \times 100 \dots (1)$$

$$\text{Surface coverage } (\theta) = \frac{W_u - W_i}{W_u} \dots (2)$$

where, ' W_u ' is the weight loss of Aluminium without inhibitor and ' W_i ' is the weight loss with inhibitor.

3.2.2. Effect of Temperature

Temperature has significant effect on the corrosion rate of metal. In order to evaluate the effect of temperature variation on corrosion and corrosion inhibition process, gravimetric measurements were further undertaken at 308 K-338 K for uninhibited and inhibited test solutions. Highest four concentrations were selected to reflect the temperature effect on corrosion inhibition. The results obtained after 60 minutes immersion reveals that with increase in temperature there is a decrease in inhibition efficiency as shown in Table 3.

Table 3: Temperature effect on the weight loss for pure Al in 1.0 M HCl for 60 minutes

Inhibitor	Concentration (g/l)	Weight loss (mgcm ⁻²)			
		308 K	318 K	328 K	338 K
Blank	-	23.685	40.43	53.03	58.08
FSE	0.469	7.317 (69.100%)	33.441 (17.286%)	45.961 (13.329%)	50.839 (12.466%)
	0.563	6.260 (73.564%)	31.246 (22.715%)	41.002 (22.681%)	49.728 (14.379%)
	0.657	6.260 (73.564%)	30.189 (25.329%)	40.596 (23.447%)	48.536 (16.432%)
	0.939	4.065 (82.834%)	28.075 (30.557%)	38.482 (27.433%)	47.614 (18.018%)

Such decrease in inhibition efficiency, suggests that the adsorption-desorption equilibrium is shifted toward desorption with increasing temperature, indicating a physical adsorption mechanism. The physisorbed inhibitor species are often perturbed and even dispersed by the increased agitation of the interface due to enhanced rates of hydrogen gas evolution at higher temperatures [20]. This tends to reduce the degree of surface coverage and inhibition efficiency even for highest concentration of inhibitor revealing that FSE is a poor inhibitor at higher temperature.

The activation energy parameter was obtained by using Arrhenius equation. In acidic solution the corrosion rate is related to temperature [21] as mentioned below:

$$\rho = K \exp\left(-\frac{E_a}{RT}\right) \dots (3)$$

where 'ρ' is corrosion rate, ' E_a ' is apparent activation energy, 'R' is molar gas constant and 'T' is the absolute temperature.

The apparent activation energy is determined for the exposure period of 1 hour as depicted in Figure 2. It has been reported that the inhibitor is said to be physisorbed over the metal surface when the value of E_a is higher in presence of inhibitor than in blank solution [22]. The result from Table 4 was in agreement with the reported work confirming adsorption type to be physisorption.

3.3. Galvanostatic polarization

The polarization curves of Al electrode after its immersion in presence and absence of inhibitor at 308 K are shown in Figure 3. The values for corrosion current densities are obtained by extrapolating the anodic and cathodic Tafel lines. These values in addition to inhibition efficiency are given in Table 5.

Table 4: Apparent activation energy for adsorption of *FSE* inhibitor on pure Al in 1.0 M HCl for exposure period of 60 minutes

Inhibitor	Concentration (g/l)	E_a KJ/mol
Blank	-	25.65
<i>FSE</i>	0.469	50.73
	0.563	53.61
	0.657	54.37
	0.939	56.87

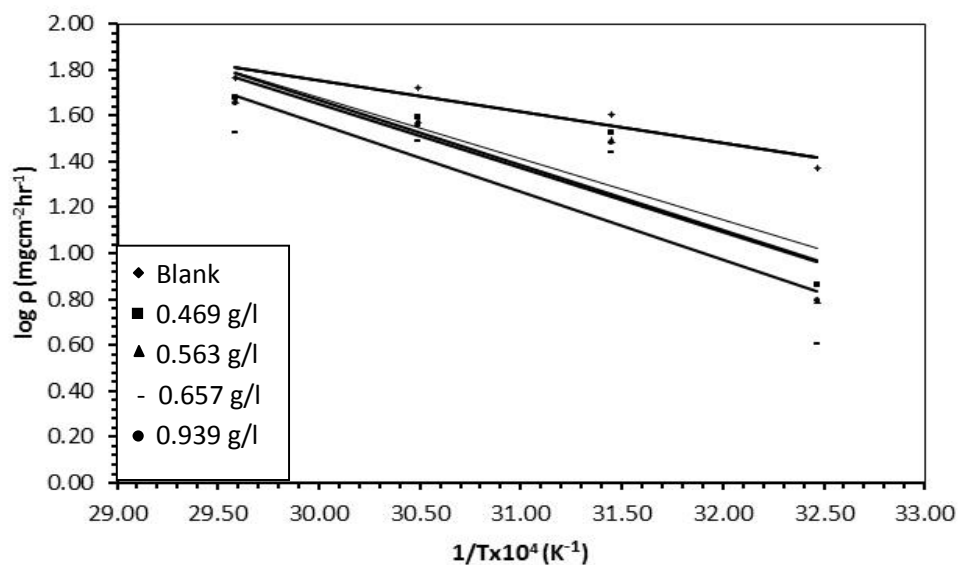
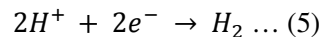


Figure 2: $\log p$ vs $1/T \times 10^4$ to calculate the apparent activation energy of corrosion process for exposure period of 60 minutes in absence and presence of *FSE*

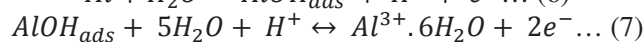
The value of I_{corr} in absence and presence of inhibitor was used to obtain the inhibition efficiency (%I.E) of the extract by using the following equation:

$$\%I.E = \frac{I_{corr}^0 - I_{corr}}{I_{corr}^0} \times 100 \dots (4)$$

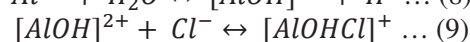
The cathode reaction for Al in HCl solution is the reduction of H^+ ion.



On the other hand anode reaction for the dissolution of Al to its cation.



The reaction is activated in presence of water and chloride ions which leads to corrosion of Al and formation of the complex [23]



Addition of *FSE* shows a decrease in the anodic and cathodic current densities compared to those recorded for the HCl solution. Results illustrate that the corrosion current density decreases with increase in concentration of inhibitor indicating protection of metal in presence of inhibitor. The corrosion potential displays a very small change from -813 mV to -830 mV versus SCE with no definite trend suggesting the inhibition to be mixed type. However, the cathodic Tafel slope (b_c) is always greater than anodic one (b_a) suggesting the predominance of

cathodic inhibition which is consistent with the results obtained from previous research [24]. Additionally, the presence of FSE shifts the cathodic and anodic branches to lower current density as compared to uninhibited one. The amount of cathodic branch shift towards lower current density is more than the anodic one with increase in concentration of inhibitor indicating the inhibition to be more of cathodic type.

Table 5: Electrochemical parameters of corrosion of pure Al in presence of different concentration of FSE at 308 K and corresponding inhibition efficiencies obtained by polarization technique

Inhibitor	Concentration (C) (g/l)	E_{corr} (mV)	b_a (mV/dec)	b_c (mV/dec)	I_{corr} for cathodic A/cm ²	I.E%
Blank	-	-820	153	200	7.760×10^{-3}	-
FSE	0.024	-821	232	373	6.166×10^{-3}	20.562
	0.094	-823	248	300	4.467×10^{-3}	42.452
	0.187	-824	270	303	4.169×10^{-3}	46.293
	0.375	-833	250	269	2.630×10^{-3}	66.113
	0.469	-826	228	281	2.455×10^{-3}	68.375
	0.563	-827	133	261	1.995×10^{-3}	74.294
	0.657	-830	207	266	1.905×10^{-3}	75.451
	0.939	-832	193	237	1.259×10^{-3}	83.781

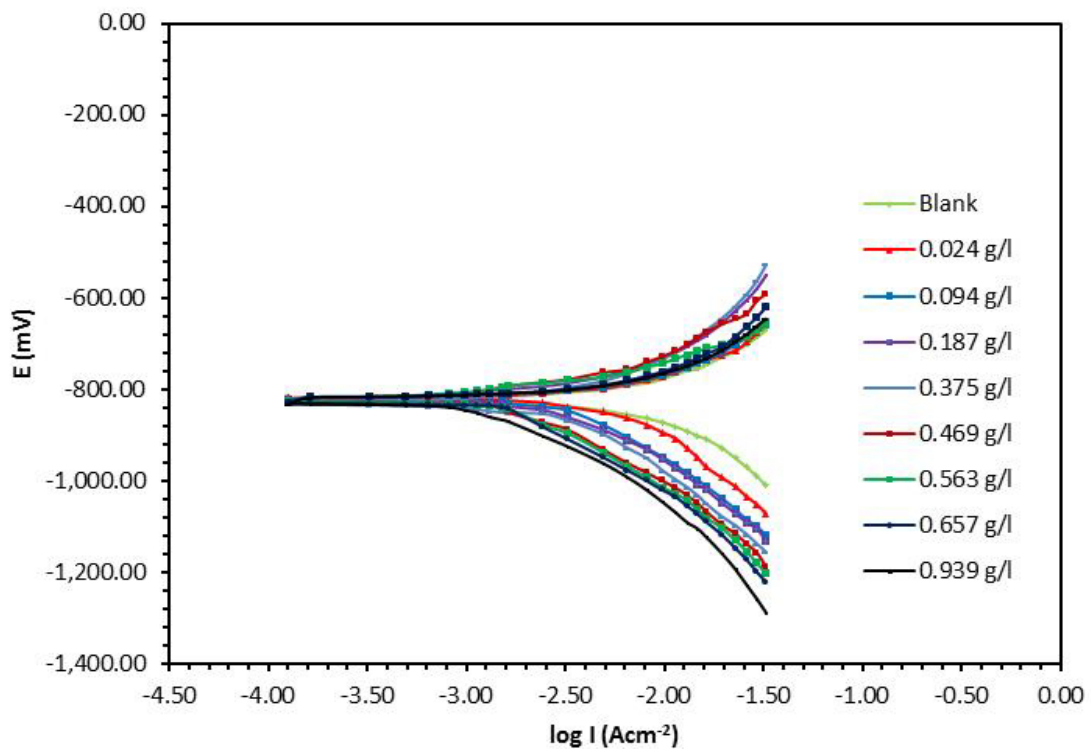


Figure 3: Anodic and cathodic polarization curves obtained from pure Al at 308 K in 1.0 M HCl in various concentration of FSE

3.4. Electrochemical impedance spectroscopy (EIS)

EIS spectra recorded at open circuit potential for the immersion period of 1 hour are characterized through Nyquist plot as depicted in Figure 4. There is a presence of depressed semicircle in Nyquist plot across the studied frequency range denoting that the dissolution process is controlled by charge transfer reaction. The reason behind the depressed semicircle in solid electrodes is attributed to frequency dispersion which can be ascribed to different physical phenomena such as surface roughness, active sites, and non-homogeneity of the solids [25].

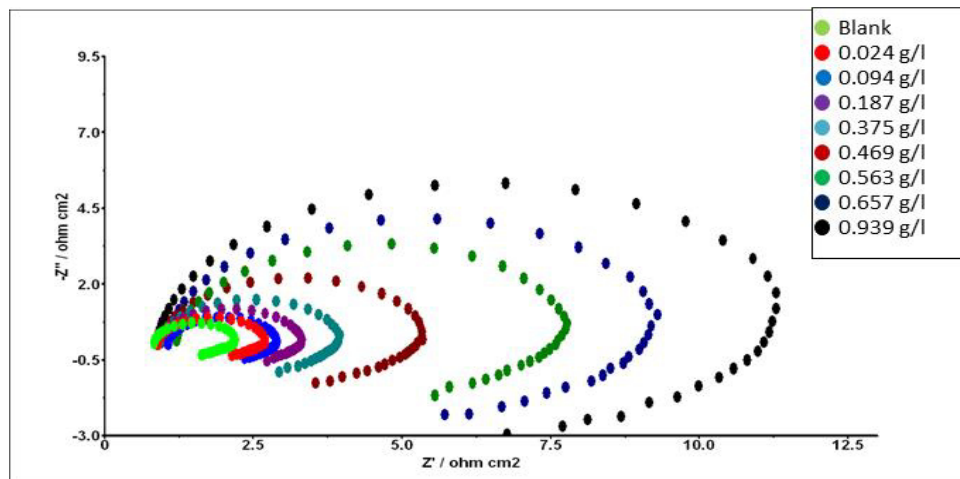


Figure 4: Impedance plot obtained at 308 K for corrosion inhibition of pure Al by FSE at various concentrations

EIS spectra are examined via fitting to the equivalent circuit model: $R_s (QR_t [LR_L])$, where R_s is solution resistance, R_t is the charge transfer resistance, Q is constant phase element (CPE) while L and R_L are inductive elements. CPE is used in place of pure capacitor for the deviations from ideal dielectric constant due to non-homogeneity on the surface of electrode and is defined by two values Q and n . The impedance of CPE is represented by:

$$Z_{CPE} = Q^{-1}(j\omega)^{-n} \quad \dots (10)$$

where $j = (-1)^{\frac{1}{2}}$, ω is frequency in rad s^{-1} , $\omega = 2\pi f$ and f is the frequency in Hz. If n equals one, the impedance of CPE is identical to that of a capacitor, $Z_C = (i\omega C)^{-1}$, and in this case Q gives a pure capacitance C . For non-homogeneous system, n ranges from 0.9–1 [26].

Since R_t value is inversely proportional to corrosion rate and hence can be used to calculate the inhibition efficiency of the inhibitor by using following equation:

$$\%I.E = \frac{R_t - R_t^0}{R_t} \times 100 \quad \dots (11)$$

Where, R_t and R_t^0 are charge transfer resistance at 1.0 M HCl in presence and absence of IVE extract, respectively. EIS parameters, listed in Table 6, illustrates that there is an increase in magnitude of R_t while decrease in that of CPE with increase in concentration of inhibitor. The behavior of R_t and Q values can be correlated with the gradual displacement of water molecules with those of the inhibitor on the electrode surface leading to a decrease in the active sites and slowing down the corrosion process. The decrease in Q values can be accredited to decline in the local dielectric constant or inflation in the thickness of the electrical double layer [26].

3.5. Adsorption isotherm

Adsorption of organic molecules occurs when the interaction energy between the inhibitor molecules and the metal surface is higher than that between the solvent molecules and the metal surface. The information on the interaction between inhibitor molecules and Al surface is provided by adsorption isotherm. There is a linear relationship between surface coverage and the concentration of inhibitor in all the isotherms. The deviation in the slope (0.92) and linear correlation coefficient (0.99) value from unity is observed when experimental data was fit in Langmuir

adsorption isotherm. The reason behind such behavior can be attributed to the interactions between adsorbate species and to the change in adsorption heat due to increasing surface coverage. Langmuir isotherm is studied by applying data obtained from gravimetric measurements to the following equation:

$$\frac{C}{\theta} = \frac{1}{K} + C \dots (12)$$

where θ is the degree of surface coverage, C (g/l) is the inhibitor concentration in solution, K is the equilibrium constant for adsorption process.

Table 6: Impedance parameters and corresponding inhibition efficiency for the corrosion inhibition of pure Al by FSE extract at 308 K

Inhibitor	Concentration (C) (g/l)	R_s (Ωcm^2)	R_t (Ωcm^2)	Q (μFcm^{-2})	R_L (Ωcm^2)	L (Hcm ²)	n	I.E. %
Blank	-	0.818	1.380	156.300	3.410	0.120	0.961	-
FSE	0.024	0.913	1.745	147.400	3.106	0.401	0.992	20.917
	0.094	1.072	1.802	130.800	2.352	0.432	0.988	23.418
	0.187	0.913	2.357	125.000	4.050	0.787	0.988	41.451
	0.375	0.927	2.991	107.100	2.836	0.651	0.972	53.861
	0.469	0.962	4.490	86.980	3.690	0.751	0.949	67.832
	0.563	1.218	6.430	77.450	8.930	1.402	0.994	78.538
	0.657	1.054	8.030	74.980	6.550	1.161	0.999	82.814
	0.939	0.905	10.250	73.130	8.760	1.769	0.998	86.536

The linear plot obtained from $\frac{C}{\theta}$ versus C graph suggest that adsorption of inhibitor follows Langmuir adsorption isotherm as depicted in Figure 5.

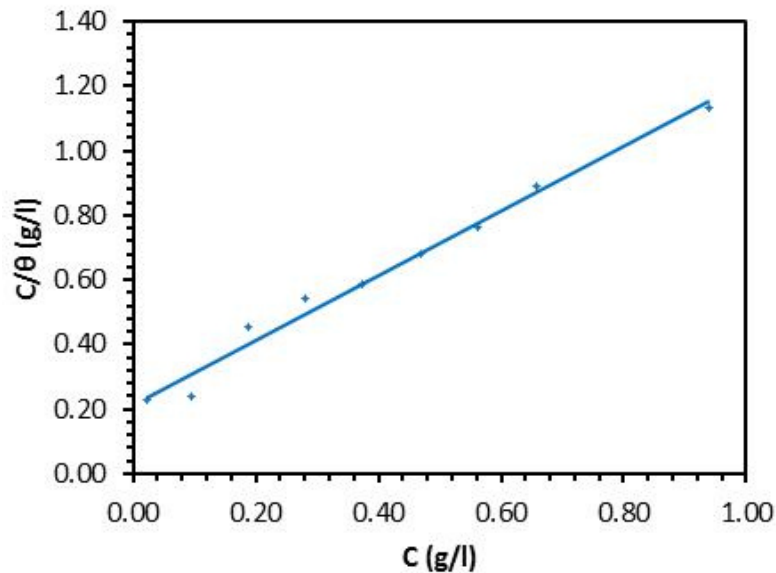
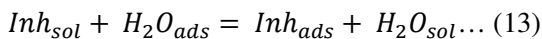


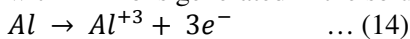
Figure 5: Langmuir adsorption isotherm plot for FSE at 35°C for 60 minutes

3.6. Mechanism of inhibition

The adsorption of the inhibitor involves replacement of water molecules which are presorbed over the metal surface.



The subscript sol and ads refers to solution and adsorption respectively. The adsorbed inhibitor may then combine with Al^{+3} ions generated in the solution to form a complex.



If the complex so formed between Al and inhibitor is stable and had no effect of external corrosive environment then the complex does not dissolve and Al is protected. However, if the complex is soluble as in case of lower concentration, the metal dissolution process is accelerated. It may be possible that at low concentration, the inhibitor molecules are insufficient to form complex with the Al leading to its dissolution. As concentration increases, more of the molecules will be available to form complex with surface of metal which subsequently diminishes solubility of the surface layer [27].

Trigonelline, IBP and Vitexin are the major chemical constituent present in *FSE* which can adsorb over the Al surface to reduce the corrosion rate. Trigonelline can donate electrons to Al through O present in its structure while positively charged N atom can also accept electron from filled s-orbital of metal. IBP and Vitexin consist of N, O and O-atoms in their structures respectively. These molecules also have the capability to donate the electrons through O, N atoms present in them while acceptance of electrons can occur due to the formation of electrophilic centers during donation of electrons.

Conclusion

The inhibitive effects *FSE* were evaluated over pure Al in 1.0 M HCl medium by using gravimetric and electrochemical techniques. The result from gravimetric method shows that inhibition efficiency increases with increase in concentration of inhibitor. However, inhibition efficiency decreases with increase in temperature indicating that the inhibitor molecules were physisorbed over the metal surface to protect it from corrosion. Al specimen was severely corroded at higher temperature indicating its ineffectiveness at higher temperature. The experimental data obtained was found to obey Langmuir adsorption isotherm. In galvanostatic polarization measurement, no significant change in the corrosion potential was observed suggesting the inhibitor to be of mixed type (cathodic as well as anodic). However, the results also reveal that the cathodic Tafel slope is higher than the anodic one indicating the predominance of cathodic inhibition. EIS measurement result displays that the constant phase element value decreases and charge transfer resistance increases with increase in concentration of inhibition. The reason for such behavior is due to adsorption of inhibitor molecule over metal/solution interface.

Acknowledgements-One of the authors, NKS, is grateful to Jawaharlal Nehru University JNU, New Delhi and UGC for providing the required facility for research. Another author, PCJ, would like to thank Central University of Gujarat for providing basic computational facilities.

References

1. Kor N.M., Didarshetaban M.B., Pour H.R.S., *Int J Adv Biol Biom Res.* 1 (2013) 922.
2. Parthasarathy V.A., Chempakam B., Zachariah T. J., *Chemistry of spices*, 2008
3. Altwaiq A.M., Khouri S.J., Al-luaibi S., Lehmann R., Drücker H., Vogt C., *J. Mater. Environ. Sci.* 2 (2011) 259
4. Benali O., Benmehdi H., Hasnaoui O., Selles C., Salghi R., *J. Mater. Environ. Sci.* 4 (2013) 127
5. Gopi D., Sherif El-Sayed M., Manivannan V., Rajeswari D., Surendiran M., Kavitha L., *Ind. Eng. Chem. Res.* 53 (2014) 4286.
6. Anejjar A., Zarrouk A., Salghi R., Zarrok H., Ben Hmamou D., Hammouti B., Elmahi B., Al-Deyab S.S., *J. Mater. Environ. Sci.* 4 (2013) 583
7. Yadav M., Kumar S., Sharma U., Yadav P.N., *J. Mater. Environ. Sci.* 4 (2013) 691
8. Reena Kumari P.D., Nayak J., Shetty A.N., *J. Mater. Environ. Sci.* 2 (2011) 387
9. Mourya P., Banerjee S., Rastogi R. B., Singh M.M., *Ind. Eng. Chem. Res.* 52 (2013) 12733.
10. Labjar N., El Hajjaji S., Lebrini M., Serghini Idrissi M., Jama C., Bentiss F., *J. Mater. Environ. Sci.* 2 (2011) 309
11. Noor E.A., *Int. J. Electrochem. Sci.* 2 (2007) 996
12. Noor E.A., *Journal of Engineering and Applied Sciences.* 3 (2008) 23.
13. Bouyanzer A., Hammouti B., Majidi L., Haloui B., *Portugaliae Electrochimica Acta* 28 (2010) 165.
14. Al-Sawaad H.Z.M., Al-Mubarak A.S.K., Haddad A.M., *J. Mater. Environ. Sci.* 1 (2010) 227
15. Oguzie E.E., Adindu C.B., Enenebeaku C.K., Ogukwe C.E., Chidiebere M.A., Oguzie K.L., *J. Phys. Chem. C.* 116 (2012) 13603.
16. Kara Y.S., Sagdin S.G., Esmé A., *Protection of Metals and Physical Chemistry of Surfaces.* 48 (2012) 710.

17. John S., Joseph A., *RSC Advances*. 2 (2012) 9944.
18. Ebenso E.E., Obot I.B., *Int. J. Electrochem. Sci.* 5(2010)2012.
19. Ozcan M., Solmaz R., Kardas G., Dehri I., *Colloids and Surfaces A: Physicochem. Eng. Aspects*. 325 (2008) 57.
20. Rahiman A.F.S.A., Sethumanickam S., *Arabian Journal of Chemistry* (2014) DOI: 10.1016/j.arabjc.2014.01.016
21. Kamal C., Sethuraman M.G., *Arabian Journal of Chemistry*. 5(2012) 155.
22. Karthikaiselvi R., Subhashini S., Rajalakshmi R., *Arabian Journal of Chemistry*. 5(2012) 517.
23. Uwah I.E., Okafor P.C., Ebiekpe V.E., *Arabian Journal of Chemistry*. 6 (2013) 285.
24. Khaled K.F., *Corrosion Science*. 52(2010) 2905.
25. Yoo S.H., Kim Y.W., Chung K., Kim N.K., Kim J.S., *Ind. Eng. Chem. Res.* 52 (2013)10880.
26. Sudheer, Quraishi M.A., *Ind. Eng. Chem. Res.* 53 (2014) 2851.
27. Al-Turkustani A. M., *Modern Applied Science*. 4 (2010) 105

(2015) ; <http://www.jmaterenvironsci.com>